

Conformational isomers of 1,2,5,6-tetrathiocins and the photoisomerization of a 1,2,5,6-tetrathiocin into a 1,2,3,6-tetrathiocin: X-ray structures of $(C_6X_4S_2)_2$ (X = F, Cl) and $C_6F_4SSSC_6F_4S$

Tristram Chivers, Masood Parvez, Ignacio Vargas-Baca, and Gabriele Schatte

Abstract: The 1,2,5,6-tetrathiocins $(C_6X_4S_2)_2$ (**3a**, X = F; **3b**, X = Cl) are obtained in high yields by the oxidation of the dithiols 1,2- $C_6X_4(SH)_2$ (X = F, Cl) with I_2 or SO_2Cl_2 , respectively. In the solid state **3a** has the C_{2h} (chair) conformation and crystallizes in two different phases: α - $(C_6F_4S_2)_2$, monoclinic, $P2_1/a$, $a = 9.351(2)$, $b = 6.465(2)$, and $c = 11.546(2)$ Å, $\beta = 95.60(1)^\circ$, $V = 694.6(2)$ Å³, $Z = 2$; and β - $(C_6F_4S_2)_2$, monoclinic, $P2_1/c$, $a = 4.825(2)$, $b = 11.302(2)$, and $c = 12.453(2)$ Å, $\beta = 91.45(3)^\circ$, $V = 678.8(3)$ Å³, $Z = 2$. By contrast, **3b** displays a D_2 (twist-boat) structure and crystallizes in the $C2/c$ space group with $a = 15.243(3)$, $b = 8.703(2)$, and $c = 27.010(14)$ Å, $\beta = 92.81(4)^\circ$, $V = 3578(1)$ Å³, and $Z = 8$. The derivative **3a** exists as an equilibrium mixture of two conformational isomers in toluene solution. The VT ^{19}F NMR data afford the thermodynamic parameters $\Delta H^\circ = 9.9 \pm 0.4$ kJ mol⁻¹ and $\Delta S^\circ = 14 \pm 1$ J K⁻¹ mol⁻¹. Density functional theory calculations for **3a** indicate that the D_2 conformation is lower in energy than the C_{2h} isomer by 4.6 kJ mol⁻¹. The photolysis of **3a** in benzene promotes a transannular sulfur migration to give the 1,2,3,6-tetrathiocin, $C_6F_4SSSC_6F_4S$ (**6**), which exists in a chair conformation with respect to antipodal sulfur atoms. Crystal structure of **6**: orthorhombic, space group $Pnma$, $a = 8.652(6)$, $b = 19.084(4)$, and $c = 8.301(6)$ Å, $V = 1370.6(14)$ Å³, and $Z = 4$. The isomers **3a** and **6** were also characterized by EI mass spectrometry, ^{19}F NMR, FTIR, and Raman spectroscopies.

Key words: tetrathiocins, conformational isomers, photoisomerization.

Résumé : Les oxydations des dithiols 1,2- $C_6X_4(SH)_2$ (X = F, Cl) par I_2 ou SO_2Cl_2 conduisent aux 1,2,5,6-tétrathiocines $(C_6X_4S_2)_2$ (**3a**, X = F; **3b**, X = Cl) avec des rendements élevés. À l'état solide, le composé **3a** adopte la conformation C_{2h} (chaise) et cristallise dans deux phases différentes: α - $(C_6F_4S_2)_2$, monoclinique, $P2_1/a$, $a = 9,351(2)$, $b = 6,465(2)$ et $c = 11,546(2)$ Å, $\beta = 95,60(1)^\circ$, $V = 694,6(2)$ Å³, $Z = 2$ et β - $(C_6F_4S_2)_2$, monoclinique, $P2_1/c$, $a = 4,825(2)$, $b = 11,302(2)$ et $c = 12,453(2)$ Å, $\beta = 91,45(3)^\circ$, $V = 678,8(3)$ Å³, $Z = 2$. Par opposition, le composé **3b** existe sous la forme D_2 (bateau-croisé) et cristallise dans le groupe d'espace $C2/c$ avec $a = 15,243(3)$, $b = 8,703(2)$ et $c = 27,010(14)$ Å, $\beta = 92,81(4)^\circ$, $V = 3578(1)$ Å³, $Z = 8$. En solution dans le toluène, le dérivé **3a** existe sous la forme d'un mélange à l'équilibre de deux isomères conformationnels. Des données de RMN du ^{19}F à TV permettent de déterminer les paramètres thermodynamiques suivants: $\Delta H^0 = 9,9 \pm 0,4$ kJ mol⁻¹ et $\Delta S^0 = 14 \pm 1$ J K⁻¹ mol⁻¹. Des calculs de densité fonctionnelle sur le composé **3a** indiquent que l'énergie de la conformation D_2 est 4,6 kJ mol⁻¹ plus faible que celle de l'isomère C_{2h} . La photolyse du composé **3a** dans le benzène provoque une migration transannulaire du soufre conduisant à la formation de la 1,2,3,6-tétrathiocine, $C_6F_4SSSC_6F_4S$ (**6**), qui existe dans une conformation chaise par rapport aux atomes de soufre antipodaux. Structure cristalline du composé **6**: orthorhombique, groupe d'espace $Pnma$, $a = 8,652(6)$, $b = 19,084(4)$ et $c = 8,301(6)$ Å, $V = 1370,6(14)$ Å³, $Z = 4$. Les isomères **3a** et **6** ont aussi été caractérisés par spectrométrie de masse sous IE, par RMN du ^{19}F et par spectroscopies FTIR et Raman.

Mots clés : tétrathiocines, isomères conformationnels, photoisomérisation.

[Traduit par la Rédaction]

Introduction

A sulfur atom (-S-) and a -CH₂- group can be viewed as isoelectronic with the important difference that, in a ring

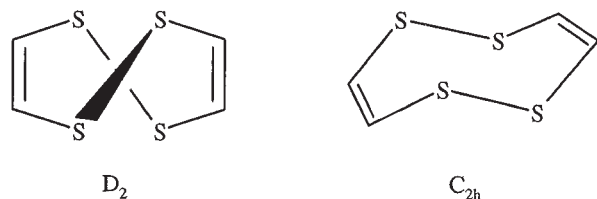
system, the exocyclic electron pairs are nonbonding for -S- but bonding for -CH₂-. Consequently, the effect that the replacement of some of the -CH₂- groups by -S- linkages has

Received February 2, 1998.

T. Chivers,¹ M. Parvez, I. Vargas-Baca, and G. Schatte. Department of Chemistry, The University of Calgary, 2500 University Drive NW, Calgary, AB T2N 1N4, Canada.

¹Author to whom correspondence may be addressed. Telephone: (403) 220-5741. Fax: (403) 289-9488. E-mail: chivers@ucalgary.ca

Scheme 1.



on the structures and conformational barriers of organic ring systems is of interest. This substitution generally facilitates the observation of interconversion by increasing the magnitude of the inversion barriers (1). Since the number of degrees of freedom and the complexity of the system increase with the number of atoms in the ring, the majority of conformational investigations has been concerned with six-membered heterocycles (2).

The study of larger rings is simplified when some atoms are constrained to remain in a plane, e.g., 1,2,5,6-tetrathiocin **1**.²

Although 3,4,7,8-tetrakis(trifluoromethyl)-1,2,5,6-tetrathiocin has been known since 1960 (3), it has not been structurally characterized. The parent ring system **1** was synthesized for the first time in 1996 (4). As in the case of cycloocta-1,5-diene (5), 1,2,5,6-tetrathiocin (**1**) should exhibit several conformers. Recent ab initio molecular orbital calculations predict that a (*Z,Z*) twist form of **1** (approximately D_2 symmetry) represents a global minimum (6) and that structure has been found in the solid state by an X-ray crystallographic analysis (Scheme 1) (4). By contrast the twist-boat form (C_2 symmetry) was calculated to be the global minimum for cycloocta-1,5-diene (5). The calculations also predict that the chair (*Z,Z*) conformation of **1** (C_{2h} symmetry) (Scheme 1) is only 22.2 kJ mol⁻¹ higher in energy than the D_2 isomer (6), and consequently, this alternative geometry should be readily accessible. Indeed the chair conformation of the C_4S_4 ring has been established for C_6S_{10} (**2a**) (7) and the related derivative (**2b**) (8).

In this article we describe the synthesis and X-ray structures of the octahalogenated derivatives **3a** and **3b**. The fluoro derivative **3a** exists as an equilibrium mixture of two conformational isomers in solution. The thermodynamic parameters for this interconversion process, obtained from variable temperature ¹⁹F NMR data, are compared with the values calculated by density functional theory (DFT) calculations. In view of the photochemical sensitivity of the parent system **1** (4), the photolysis of **3a** was also investigated.

Experimental section

Reagents and general procedures

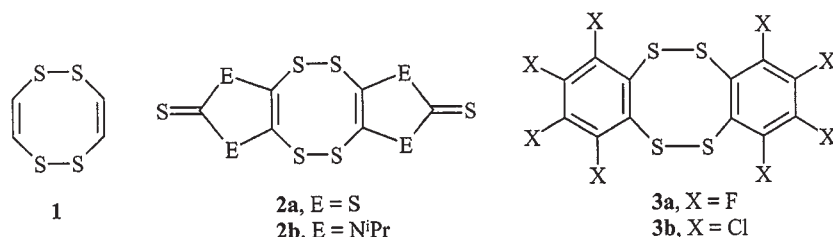
All solvents were dried by treatment with the appropriate drying agent and freshly distilled before use. 1,2,3,4-Tetrafluorobenzene, C_6Cl_6 , *n*-BuLi (2.5 M solution in hexanes), $Na_2S \cdot 9H_2O$, and I_2 were commercial reagents used as received. The SO_2Cl_2 was distilled under an N_2 atmosphere before use. Sulfur was recrystallized from CS_2 . Tetrafluorobenzene-1,2-dithiol, $C_6F_4-1,2-(SH)_2$ (bp 50°C, 5×10^{-2} Torr (1 Torr = 133.3 Pa); ¹H NMR ($CDCl_3$), δ : 3.82; ¹⁹F NMR ($CDCl_3$): -131.7 (m) and -158.5 (m)) was obtained in 70% yield by the literature method (9). The $C_6Cl_4-1,2-(SH)_2$ was prepared by a modification (vide infra) of the literature method (10). The $(C_6F_4S)_2$ was also synthesized by a known procedure (11).

Instrumentation

The ¹H NMR spectra were obtained on a Bruker ACE 200 MHz spectrometer, and chemical shifts are reported in ppm relative to Me_4Si . The ¹⁹F NMR spectra were recorded on a Bruker AMX 300 spectrometer; chemical shifts are reported relative to $CFCl_3$ and were measured with an external standard of C_6F_6 (δ -162.9 ppm). Electron impact mass spectra were obtained by using a VG Micromass spectrometer (VG 7070) set at 70 eV. The FTIR spectra were recorded as Nujol mulls (KBr plates) on a Mattson 4030 FTIR spectrometer in the range 4000–300 cm⁻¹ (resolution: 4 cm⁻¹; number of scans: 128). Raman spectra were recorded using a Jarrell–Ash model 25-100 monochromator interfaced to a microcomputer. A Coherent Radiation Model 540 argon laser fitted with an Innova 70 plasma tube was used as the exciting source (emission wavelength: 514.5 nm; laser power: 100 mW; laser current: 30 A). Scattered radiation was collected at 90° to the incident light. The Raman spectra were obtained from neat samples sealed in melting point tubes and measured in the range 2500–100 cm⁻¹ at room temperature. The frequencies are believed accurate to ± 2 cm⁻¹. Elemental analyses were performed by Canadian Microanalytical Service Ltd., Vancouver, B.C., and by Galbraith Laboratories Inc., Knoxville, Tennessee.

Preparation of $C_6Cl_4-1,2-(SH)_2$

In a typical preparation C_6Cl_6 (32.7 g, 0.11 mol), Fe powder (6.2 g, 0.11 mol) and $Na_2S \cdot 9H_2O$ (54 g, 0.22 mol) were heated at reflux in DMF (1 L) for 48 h. **Caution:** a wide-necked condenser and vigorous reflux are necessary to prevent sublimed C_6Cl_6 from plugging the condenser and



²1,2,5,6-Tetrathiacycloocta-3,7-diene.

causing a pressure build-up. The mixture was allowed to cool to 23°C and then 2 L of NaOH (0.75 M) were added with vigorous stirring. The mixture was allowed to settle (48 h) and then centrifuged to separate the solid, which was dissolved in 300 mL of MeOH and refluxed for 3 h with ZnO (8 g) and NaOH (150 mL, 0.75 M). The hot slurry was filtered, and the solution was acidified to a neutral pH with H₂SO₄. A pale-yellow precipitate was filtered and dried with an air stream in the filtration funnel. This product was extracted (Soxhlet apparatus) with Et₂O to remove a dark-green insoluble material. The solvent was evaporated from the solution to leave 11.3 g of a yellow solid. This crude product was shown by EIMS to consist of a mixture of C₆Cl₅SH and C₆Cl₄-1,2-(SH)₂ (yield ~36%). Recrystallization from toluene and subsequent sublimation (140°C, 5 × 10⁻² torr) produced C₆Cl₄-1,2-(SH)₂ containing only traces of C₆Cl₅SH.

Preparation of (C₆F₄S₂)₂ (**3a**)

A solution of C₆F₄-1,2-(SH)₂ (1.66 g, 7.70 mmol) in methanol (50 mL) was treated with a solution of I₂ (1.97 g, 7.70 mmol) in methanol (50 mL). A pale-yellow, microcrystalline product was formed. The crude product was filtered, rinsed with cold methanol, and recrystallized from Et₂O to give (C₆F₄S₂)₂ (**3a**) (1.42 g, 3.32 mmol, 86%); mp 193°C. Anal. calcd. for C₆F₄S₂: C 33.96, F 35.82, S 30.23; found: C 33.81, F 33.85, S 30.55.³

EIMS (*m/z*, %): 424, 40 (M⁺), 328, 15 (C₁₂F₈S⁺), 212, 100 (C₆F₄S₂⁺), 168, 38 (C₅F₄S⁺). ¹⁹F NMR (CDCl₃, δ): two sets of resonances at -130.1 (m), -154.4 (m) and -122.1 (m), -147.4 (m) with approximate relative intensities 1:4. IR (Nujol, cm⁻¹): 1594 m, 1307 s, 1237 s, 1038 s, 973 m, 872 s, 818 s, 724 s, 483 w, 414 s.

Preparation of (C₆Cl₄S₂)₂ (**3b**)

A solution of SO₂Cl₂ (0.67 g, 5.0 mmol) in benzene (10 mL) was added to a solution of C₆Cl₄-1,2-(SH)₂ (1.33 g, 4.75 mmol) in benzene (50 mL). After 1 h the solvent was decanted by cannula to leave a yellow solid, which was rinsed with pentane (2 × 10 mL) to give (C₆Cl₄S₂)₂ (**3b**) (1.18 g, 2.12 mmol, 90%); mp 290°C (dec.). Anal. calcd. for C₆Cl₄S₂: C 25.92, Cl 51.01, S 23.07; found: C 26.30, Cl 48.88, S 23.27.³ EIMS (*m/z*): 556 (M⁺). IR (Nujol, cm⁻¹): 1377 s, 1335 m, 1303 s, 1095 m, 869 m.

Photoisomerization of **3a**

A solution of **3a** (0.60 g, 1.41 mmol) in benzene (50 mL) in a Pyrex vessel at 23°C was irradiated with a Hg lamp. The progress of the reaction was monitored by ¹⁹F NMR spectroscopy. After 7 h, solvent was removed under vacuum and the pale-yellow product was recrystallized from CH₂Cl₂-hexane to give C₆F₄SSSC₆F₄S (**6**) (0.35 g) contaminated with **3a** (¹⁹F NMR). A pure sample of **6** was ob-

tained as a white solid by vacuum sublimation at 90°C and 10⁻³ Torr; mp 116–117°C. Anal. calcd. for C₆F₄S₂: C 33.96, S 30.23; found: C 33.53, S 32.10.³ EIMS (*m/z* %): 424, 30 (M⁺), 392, 26 (C₁₂F₈S₃⁺), 360, 40 (C₁₂F₈S₂⁺), 328, 100 (C₁₂F₈S⁺), 244, 20 (C₆F₄S₃⁺), 212, 100 (C₆F₄S₂⁺), 180, 37 (C₆F₄S⁺), 168, 40 (C₅F₄S⁺); ¹⁹F NMR (CDCl₃, δ): -117.3 (m), -122.9 (m), -147.5 (m), -147.8 (m). IR (Nujol, cm⁻¹): 1600 (s), 1487 (vs), 1305 (s), 1237 (s), 1163 (s), 1115 (s), 1042 (vs), 970 (m), 951 (m, sh), 866 (s), 817 (s), 771 (m), 724 (s), 491 (m), 446 (m).

X-ray diffraction studies

All measurements were made on a Rigaku AFC6S diffractometer using graphite monochromated Mo-K_α radiation. Crystallographic data for α-**3a**, β-**3a**, **3b**, and **6** are given in Table 1.⁴

α-**3a**

A yellow hexagonal-plate crystal of α-(C₆F₄S₂)₂ was mounted on a glass fibre. Cell constants and an orientation matrix for data collection, obtained from a least-squares refinement using the setting angles of 17 carefully centred reflections in the range 30.00 < 2θ < 50.00°, corresponded to a primitive monoclinic cell. The data were corrected for Lorentz, polarization, and empirical absorption effects (12). The structure was solved by direct methods (13) and expanded using Fourier techniques (14). All non-hydrogen atoms were refined anisotropically. All calculations were performed using the teXsan crystallographic software package (15).

β-**3a**

A yellow prismatic crystal of β-(C₆F₄S₂)₂ was mounted on a glass fibre. Cell constants and an orientation matrix for data collection, obtained from a least-squares refinement using the setting angles of 13 carefully centred reflections in the range 40.00 < 2θ < 50.00°, corresponded to a primitive monoclinic cell. The structure was solved by direct methods (16) and expanded using Fourier techniques (14). The rest of the calculations involving data processing and structure refinement followed the same procedures as described for α-**3a**.

3b

An orange prismatic crystal of (C₆Cl₄S₂)₂ was mounted on a glass fibre. Cell constants and an orientation matrix for data collection, obtained from a least-squares refinement using the setting angles of 25 carefully centred reflections in the range 15.00 < 2θ < 30.00°, corresponded to a C-centred monoclinic cell. Based on the systematic absences *hkl*, *h + k* ≠ 2*n* and *h0l*, *l* ≠ 2*n*, packing considerations, a statistical analysis of intensity distribution, and the successful solution and refinement of the structure, the space group was deter-

³Consistently low analyses for halogens were obtained for both **3a** and **3b** by two different commercial analysts. Low analyses for fluorine were also obtained for **6**.

⁴Crystal data, tables of atomic coordinates and displacement parameters, complete listings of bond lengths and angles, and other refinement data may be purchased from: The Depository of Unpublished Data, Document Delivery, CISTI, National Research Council of Canada, Ottawa, Canada, K1A 0S2. Crystal data, atomic coordinates, and bond lengths and angles have also been deposited with the Cambridge Crystallographic Data Centre and can be obtained on request from: The Director, Cambridge Crystallographic Data Centre, University Chemical Laboratory, 12 Union Road, Cambridge, CB2 1EZ, U.K.

Table 1. Crystallographic data for $(C_6X_4S_2)_2$ ($X = F, Cl$) and $\overline{C}_6F_4SSSC_6F_4S$.

	α - 3a	β - 3a	3b	6
Dimensions (mm)	0.60 × 0.50 × 0.15	0.50 × 0.27 × 0.24	0.30 × 0.27 × 0.10	0.40 × 0.30 × 0.20
Formula	α - $C_{12}F_8S_4$	β - $C_{12}F_8S_4$	$C_{12}Cl_8S_4$	$C_{12}F_8S_4$
fw	424.36	424.36	556.00	424.36
Space group	$P2_1/a$	$P2_1/c$	$C2/c$	$Pnma$
a (Å)	9.351(2)	4.825(2)	15.243(3)	8.652(6)
b (Å)	6.465(2)	11.302(2)	8.703(2)	19.084(4)
c (Å)	11.546(2)	12.453(2)	27.010(14)	8.301(6)
β (°)	95.60(1)	91.45(3)	92.81(4)	—
V (Å ³)	694.6(2)	678.8(3)	3578(1)	1370.6(14)
Z	2	2	8	4
T (°C)	-103.0	-123.0	-103.0	-103.0
λ (Å)	0.71069	0.71069	0.71069	0.71069
ρ_{calcd} (g cm ⁻³)	2.029	2.076	2.064	2.056
μ (cm ⁻¹)	7.42	7.89	17.17	7.81
Reflections: Collected	1440	1427	3557	1443
Unique	1356	1272	3413	1443
Observed	1022	912	1666	1252
Criteria	$I > 3.0\sigma(I)$	$I > 3.0\sigma(I)$	$I > 3.0\sigma(I)$	$I > 2.0\sigma(I)$
Transmission factors	0.803–1.00	0.972–1.00	0.786–1.000	0.918–1.000
Coefficients used	F	F	F	F_2
R, R_w	0.033, ^a 0.033 ^b	0.025, ^a 0.024 ^b	0.047, ^a 0.045 ^b	0.032, ^a 0.077 ^c
p -Factor	0.005	0.010	0.008	—
Goodness of fit, S	3.84	1.88	1.82	1.22
Max shift/error	0.00	0.00	0.17	0.00
Max and min peaks	0.37	0.26	0.65	0.37
In final diff. map	-0.25	-0.25	-0.52	-0.33

^a $R = \sum(|F_o| - |F_c|) / \sum|F_o|$.

^b $R_w = [\sum w(|F_o| - |F_c|)^2 / \sum w F_o^2]^{1/2}$, where $w = 1/\sigma^2(F_o) = 4F_o^2/\sigma^2(F_o^2)$ and $\sigma^2(F_o^2) = \{S^2(C+R^2B) + (pF_o^2)^2\}/Lp^2$, S = scan rate, C = total integrated peak count, R = ratio of scan time to background counting time, B = total background count, Lp = Lorentz-polarization factor, p = p -factor.

^c $R_w = [\sum w(|F_o| - |F_c|)^2 / \sum w F_o^2]^{1/2}$, where $w = 1/[\sigma_2(F_o)^2 + (0.037P)^2 + 0.610P]$, $P = (F_o^2 + 2F_c^2)/3$.

mined to be $C2/c$ (no. 15). The data processing, structure solution, and refinement followed the same procedures as described for α -**3a**.

6

A colourless, plate-like crystal of $\overline{C}_6F_4SSSC_6F_4S$ was mounted on a glass fibre. Cell constants and an orientation matrix for data collection, obtained from a least-squares refinement using the setting angles of 25 carefully centred reflections in the range $18.21 < 2\theta < 21.43^\circ$, corresponded to a primitive orthorhombic cell. Based on the systematic absences of $0kl$, $k + 1 = 2n + 1$ and $hk0$, $h = 2n + 1$, packing considerations, a statistical analysis of intensity distribution, and the successful solution and refinement of the structure, the space group was determined to be $Pnma$ (no. 62). The structure was solved by direct methods (16) and expanded using Fourier techniques (14). The structure was refined with the aid of SHELX93 (17). Other details of the structure refinement were similar to those described for β -**3a**.

Computational details

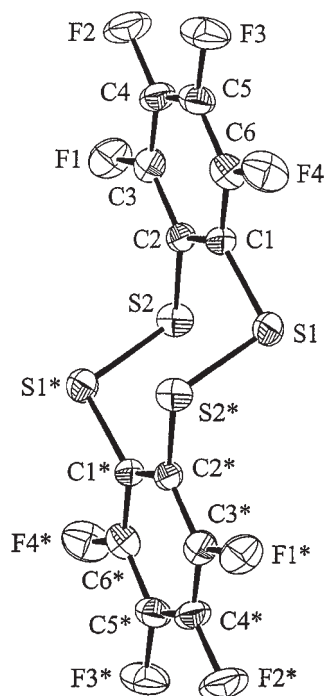
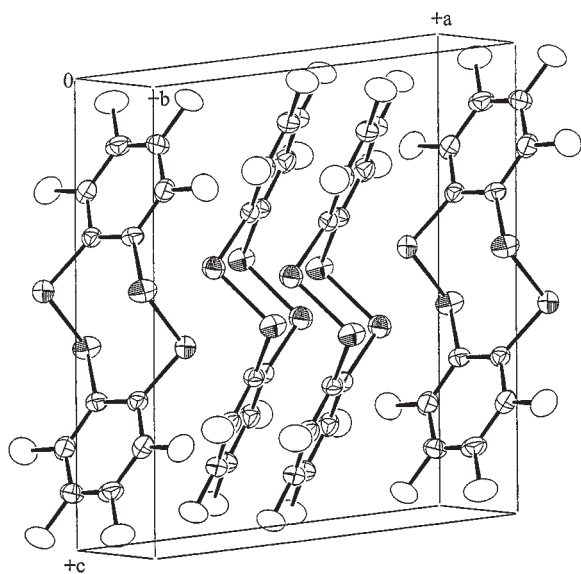
Details of the methods used for the DFT calculations can be found in ref. 18.

Results and discussion

Synthesis and X-ray structures of dibenzotetrathiocins **3a** and **3b**

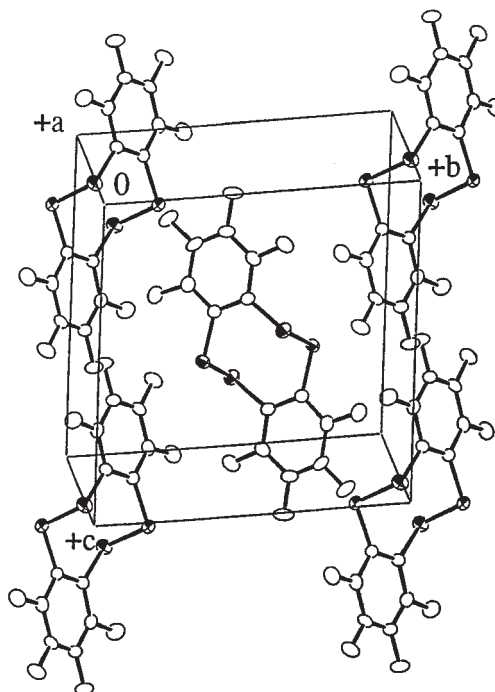
The tetrathiocins $(C_6F_4S_2)_2$ (**3a**) and $(C_6Cl_4S_2)_2$ (**3b**) were prepared by the oxidation of the corresponding dithiols with I_2 or SO_2Cl_2 , respectively, in >85% yields. Compounds **3a** and **3b** are air stable, pale-yellow solids with high thermal stability. They are also stable in polar solvents, e.g., acetonitrile or chloroform. For comparison, the parent tetrathiocin (**1**), which is obtained in only 14% yield by the oxidation of *cis*-disodium ethene-1,2-dithiolate, is converted to the tetramer $(-CH=CH-S-S-)_4$ in acetonitrile at room temperature (4).

Single crystals of **3a** were grown from a diethyl ether solution. Two different crystalline phases, which could be separated manually, were apparent. The most abundant (α -**3a**) consists of hexagonal plates, while the other phase (β -**3a**) forms rectangular prisms. X-ray diffraction analysis reveals that the chair conformer (C_{2h}) of the 1,2,5,6-tetrathiocin ring pertains in both types of crystals (see Fig. 1). The difference between the α and β phases is caused by distinctive packing arrangements (see Figs. 2 and 3). A chair conformation for the 1,2,5,6-tetrathiocin ring has also been observed for **2a** (7) and **2b** (8). By contrast, crystals of **3b**, obtained by slow evaporation of a very dilute THF solution, provided an

Fig. 1. The ORTEP diagram for $(C_6F_4S_2)_2$ (**3a**).**Fig. 2.** Packing diagram for the α crystalline phase of $(C_6F_4S_2)_2$ (**3a**).

X-ray structure corresponding to the known twist-boat conformation (D_2) of the tetrathiocin ring **1** (4) (see Fig. 4).

Relevant molecular dimensions for **3a** and **3b** are summarized in Tables 2 and 3. The mean bond distances and bond angles in the two dibenzotetrathiocins are very similar ($d(C-C) = 1.40$ Å, $d(C-S) = 1.77$ Å, $d(S-S) = 2.05$ Å, $[\text{angle CCS}] = 124.3^\circ$, $[\text{angle CSS}] = 103.8^\circ$). For comparison, the corresponding values for the parent compound **1** are 1.33 Å, 1.75 Å, 2.06 Å, 129.0° , and $104.8^\circ(4)$. The benzo-dithiolato units in **3a** and **3b** are nearly planar, with S-C-C-S and S-C-C-C torsion angles close to 0° and 180° ,

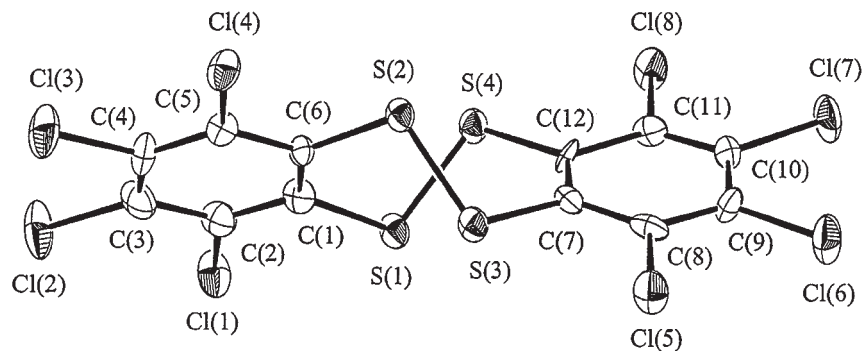
Fig. 3. Packing diagram for the β crystalline phase of $(C_6F_4S_2)_2$ (**3a**).

respectively. The C-S-S-C torsion angles are ca. 111° for **3a** and $115.3(4)^\circ$ and $118.2(4)^\circ$ for **3b**. The major disparity resulting from the different ring conformations of **3a** and **3b** is in the S-S-C-C torsion angles, which are 79.9° for **3a** and $42.3-52.2^\circ$ for **3b**.

Conformational isomers of **3a**

The ^{19}F NMR spectrum of **3a** in toluene solution at 300 K displays four resonances. These can be separated into two pairs, on the basis of their relative intensities. The less intense pair of AA'XX' multiplets is centred at $\delta -130.7$ and -154.7 ppm, while the more intense pair appears at $\delta -123.3$ and -148.3 ppm. These observations suggest that **3a** exists as a mixture of the C_{2h} and D_2 conformers in solution (see Table 4). The interconversion of these two conformational isomers in toluene solution was investigated by variable temperature ^{19}F NMR spectroscopy. The relative intensity of the two pairs of resonances changes reversibly within the temperature range 300–380 K, as a result of the equilibrium between the two conformers. However, no significant line broadening or chemical-shift changes were observed, indicating that the fluxional process is too slow to be observed on the NMR time scale. The equilibrium constants at different temperatures were obtained from the intensity ratios for the two pairs of resonance (see Table 5) and a plot of $\ln K$ vs. T^{-1} (see Fig. 5) was used to determine ΔH° and ΔS° for this process. The experimental value of ΔH° is 9.9 ± 1 kJ mol $^{-1}$. The ΔS° value of 14 ± 1 J K $^{-1}$ can be attributed primarily to changes in solvation.

In view of the apparent inversion of the order of stability of the C_{2h} and D_2 conformers for **3a** compared to that calculated for **1** (6), the energies of these two conformers were determined by density functional theory calculations. The structure of **3a** was fully optimised for both C_{2h} and D_2 sym-

Fig. 4. The ORTEP diagram for $(C_6Cl_4S_2)_2$ (**3b**).**Table 2.** Selected bond distances (Å), bond angles ($^\circ$), and torsion angles ($^\circ$) for $(C_6F_4S_2)_2$ (**3a**).^a

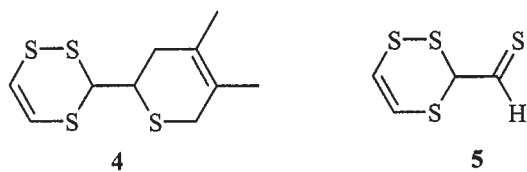
	α	β
S(1)—S(2)*	2.057(1)	2.064(1)
S(1)—C(1)	1.771(3)	1.771(3)
C(1)—C(2)	1.403(4)	1.409(4)
S(2)—C(2)	1.771(3)	1.772(3)
S(2)*-S(1)-C(1)	103.0(1)	102.73(9)
S(1)-C(1)-C(2)	123.1(2)	123.1(2)
S(1)*-S(2)-C(2)	102.8(1)	102.97(9)
S(2)-C(2)-C(1)	123.5(3)	123.6(2)
S(1)*-S(2)-C(2)-C(1)	83.1 (3)	79.9(2)
S(1)-C(1)-C(2)-C(3)	-177.9(3)	176.1(2)
C(1)-S(1)-S*(2)-C*(2)	111.4(2)	-111.3(1)
S(1)-C(1)-C(2)-S(2)	-2.1(4)	-1.8(3)
S(2)-C(2)-C(1)-C(6)	174.7(3)	-179.6(2)

^a Starred atoms are related to the unstarred atoms by symmetry operation: $x, 1/2 - y, z$.

Table 3. Selected bond distances (Å), bond angles ($^\circ$), and torsion angles ($^\circ$) for $(C_6Cl_4S_2)_2$ (**3b**).

S(1)—S(4)	2.033(3)	S(2)—S(3)	2.042(3)
S(1)—C(1)	1.782(8)	S(2)—C(6)	1.783(9)
S(3)—C(7)	1.799(8)	S(4)—C(12)	1.772(8)
C(1)—C(6)	1.40(1)	C(7)—C(12)	1.40(1)
S(1)-C(1)-C(6)	125.2(7)	S(2)-C(6)-C(1)	124.8(6)
S(3)-C(7)-C(12)	123.5(7)	S(4)-C(12)-S(7)	127.3(6)
S(4)-S(1)-C(1)	104.7(3)	S(3)-S(2)-C(6)	102.7(3)
S(1)-S(4)-C(12)	104.5(3)	S(2)-S(3)-C(7)	104.4(3)
S(4)-S(1)-C(1)-C(6)	-48.7(9)	S(3)-S(2)-C(6)-C(1)	-52.2(8)
S(2)-S(3)-C(7)-C(12)	-42.3(8)	S(1)-S(4)-C(12)-C(7)	-42.4(9)
S(1)-C(1)-C(6)-S(2)	3(1)	S(3)-C(7)-C(12)-S(4)	-7(1)
S(1)-C(1)-C(6)-C(5)	-178.1(7)	S(2)-C(6)-C(1)-C(2)	-178.8(7)
S(3)-C(7)-C(12)-C(11)	171.9(7)	S(4)-C(12)-C(7)-C(8)	171.9(7)
C(1)-S(1)-S(4)-C(12)	115.3(4)	C(6)-S(2)-S(3)-C(7)	118.2(4)

metries. The molecular dimensions were in agreement with the experimental values for **3a** and **3b** to within 0.01 Å for bond distances, 1° for bond angles, and 5° for torsional an-



gles. The calculations indicate that the D_2 conformer should be the most stable in this case, but the difference of total energies of the two conformers is only 4.6 kJ mol^{-1} , significantly less than the value of 22.2 kJ mol^{-1} estimated for **1** (**6**).

Photolysis of octafluorodibenzo-1,2,5,6-tetrathiocin (**3a**)

The parent ring system **1** is photochemically sensitive even towards daylight (**4**). The photolysis of **1** in benzene solution in the presence of excess 2,3-dimethylbutadine

Table 4. The ^{19}F NMR chemical shifts (in ppm) for $(\text{C}_6\text{F}_4\text{S}_2)_2$ and $(\text{C}_6\text{F}_4\text{S}_2)_2$ isomers.

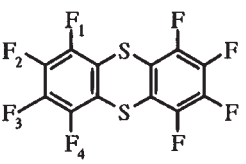
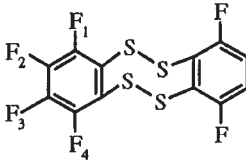
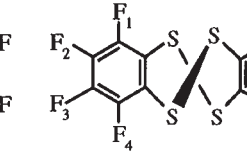
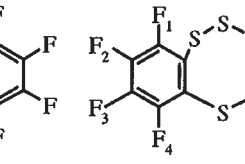
				
F_1 :	-134	-130.1	-122.1	-117.3
F_2 :	-155	-154.4	-147.4	-147.5
F_3 :	-155	-154.4	-147.4	-147.8
F_4 :	-134	-130.1	-122.1	-122.9
Reference:	11	This work	This work	This work

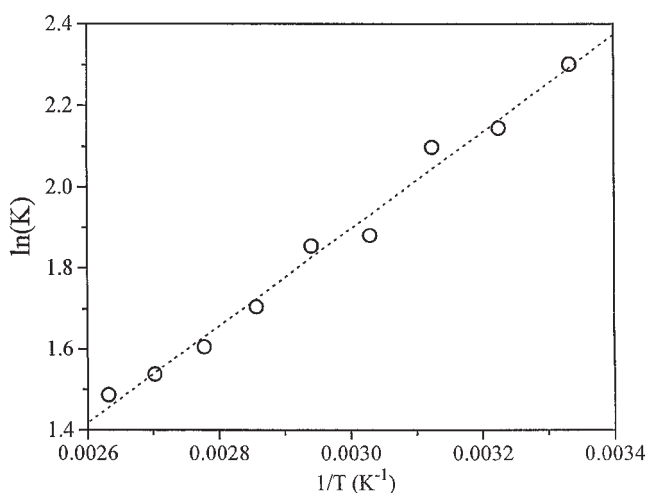
Table 5. Measured conformational equilibrium constant for $(\text{C}_6\text{F}_4\text{S}_2)_2$ (**3a**) at different temperatures.

T (K)	K
300	9.99
310	8.55
320	8.16
330	6.55
340	6.38
350	5.51
360	4.98
370	4.65
380	4.42

produced the bicyclic product **4** in 62% yield, suggesting the intermediate formation of the thioaldehyde **5**.

In view of these observations it was of interest to determine the influence of the rigid benzo substituents in **3a** on the outcome of the photochemical transformation. A solution of **3a** in benzene in a Pyrex vessel was irradiated with a medium-pressure mercury lamp through a Pyrex filter. The reaction was monitored by ^{19}F NMR, which revealed the formation of an intermediate with resonances at δ -121.8, -123.3, -146.7, and -147.1. The final product was identified as octafluorodibenzo-1,2,3,6-tetrathiocin (**6**) by elemental analysis, EIMS, ^{19}F NMR, IR, and Raman spectra, and by an X-ray structure (vide infra).

The photoisomerized product **6** is readily distinguished from the isomers of **3a** by the ^{19}F NMR spectrum, which exhibits an AMXY pattern (Table 4). The multiplets attributed to the inequivalent *ortho*-fluorine atoms have significantly different chemical shifts whereas those assigned to the other pair of inequivalent fluorine atoms differ by only 0.3 ppm. The mass spectra of **3a** and **6** show major differences. Both compounds exhibit the molecular ion $\text{C}_{12}\text{F}_8\text{S}_4^+$ with similar intensities. However, the mass spectrum of **6** also exhibits

Fig. 5. Temperature dependence of the conformational equilibrium constant for $(\text{C}_6\text{F}_4\text{S}_2)_2$ (**3a**).

increasingly high abundances of the ions $[\text{C}_{12}\text{F}_8\text{S}_3]^+$ and $[\text{C}_{12}\text{F}_8\text{S}_2]^+$, suggesting that loss of sulfur (from the S_3 chain) is the dominant fragmentation process, which leads to the parent ion $[\text{C}_{12}\text{F}_8\text{S}^+]$. By contrast, the parent ion for **3a** is the monomeric fragment $\text{C}_6\text{F}_4\text{S}_2^+$, indicating that cleavage of *both* disulfide bonds occurs predominantly in this case.

Raman spectroscopy is a diagnostic technique for the identification of SS vibrations, which are normally observed in the 450–550 cm^{-1} region (19). In the present work, the photoisomerized product **6** should be readily distinguished by the presence of both asymmetric and symmetric stretching vibrations for the trisulfide (S_3) unit, whereas the precursor **3a** will exhibit only $\nu_s(\text{SS})$. Consistently, the Raman spectrum of **6** shows bands at 492 and 469 cm^{-1} . On the basis of its stronger intensity, the former is attributed to $\nu_s(\text{SSS})$ (cf. HSSSH (20)). The Raman spectrum of **3a** exhibits only one band in the 450–550 cm^{-1} region at 497 cm^{-1} , which is assigned to $\nu_s(\text{SS})$ (cf. 489 cm^{-1} for $\text{C}_6\text{F}_5\text{SSC}_6\text{F}_5$ (21)).

[1]

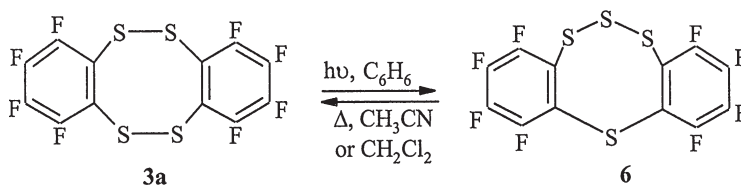
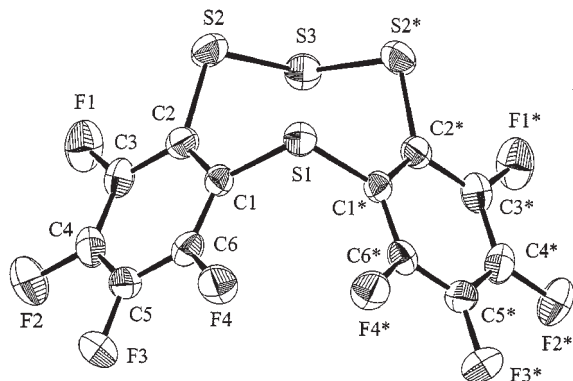
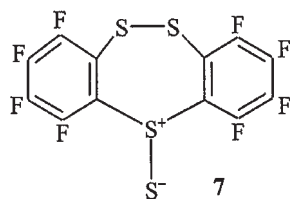


Fig. 6. The ORTEP diagram for $\overline{C_6F_4SSSC_6F_4S}$ (**6**).



The photochemical transformation of **3a** into **6** (eq. [1]) formally involves a transannular migration of a sulfur atom. In view of the similarity of the ^{19}F NMR spectra of **6** and the intermediate observed in this process (vide supra), it is suggested that this intermediate is a conformational isomer of **6**. A similar isomerization of a C_4S_4 ring has been reported for C_6S_{10} (**2a**) but, in that example, the transformation from a 1,2,5,6- to a 1,2,3,6-tetrathiocin involves a Hg^{2+} -promoted hydrolysis to give $\text{C}_6\text{S}_8\text{O}_2$ (**22a**). A mechanism involving a thiosulfoxide intermediate has been proposed for the sulfur transfer process (**22b**). Although organic



thiosulfoxides R_2SS have not been characterized, the SS double bond is known to be stabilized by electronegative groups (23). For example, the cyclic thiosulfite $\text{ROS}(=\text{S})\text{OR}$ (R = cyclohexylidene) is stable at 20°C (24). In the case of the transformation represented by eq. [1], the proposed intermediate **7** may be stabilized by the electronegative perfluoroaryl groups attached to sulfur. Finally, we note that **6** is unstable in solution in polar solvents and slowly reverts to **3a**.

X-ray structure of octafluorodibenzo-1,2,3,6-tetrathiocin (**6**)

The structure of **6** was established by X-ray crystallography. An ORTEP diagram is represented in Fig. 6, and relevant structural parameters are given in Table 6. The $\text{S}-\text{S}$ bond length of $2.047(1)$ Å is, as expected, a typical single-bond value. The bond angle $\text{S}-\text{S}-\text{S} = 107.2(1)^\circ$ is close to the mean value of 107.9° reported for *cyclo*-octasulfur (21). However, the mean bond distance, $d(\text{C}-\text{S}) = 1.79$ Å, and mean bond angles, $|\text{angle CCS}| = 122.6^\circ$, $|\text{angle CSS}| = 103.1^\circ$, show small, but significant, differences from the corresponding values for **3a** and **3b**, possibly owing to slightly greater ring strain in **6**. The small bond angle $\text{C}(1)-\text{S}(1)-\text{S}(1)^*$ of $102.81(1)^\circ$ is perhaps indicative of some ring strain. The C_4S_4 ring in **6** adopts a chair conformation with respect to the sulfur atoms $\text{S}(1)$ and $\text{S}(3)$. The value of

Table 6. Selected bond distances (Å), bond angles ($^\circ$), and torsion angles ($^\circ$) for $\overline{C_6F_4SSSC_6F_4S}$ (**6**).^a

$\text{S}(1)-\text{C}(1)$	1.799(2)
$\text{S}(2)-\text{C}(2)$	1.782(2)
$\text{S}(2)-\text{S}(3)$	2.047(1)
$\text{S}(1)-\text{C}(1)-\text{C}(2)$	121.7(1)
$\text{C}(1)-\text{C}(2)-\text{S}(2)$	123.5(1)
$\text{C}(2)-\text{S}(2)-\text{S}(3)$	103.1(1)
$\text{S}(2)-\text{S}(3)-\text{S}(2)^*$	107.2(1)
$\text{C}(1)-\text{S}(1)-\text{C}(1)^*$	102.8(1)
$\text{C}(2)-\text{S}(2)-\text{S}(3)-\text{S}(2)^*$	-93.78(10)
$\text{C}(1)^*-\text{S}(1)-\text{C}(1)-\text{C}(2)$	-94.94(13)
$\text{C}(1)^*-\text{S}(1)-\text{C}(1)-\text{C}(6)$	85.01(14)
$\text{S}(1)-\text{C}(1)-\text{C}(2)-\text{C}(3)$	179.95(15)
$\text{S}(1)-\text{C}(1)-\text{C}(2)-\text{S}(2)$	-6.0(2)
$\text{S}(3)-\text{S}(2)-\text{C}(2)-\text{C}(3)$	-103.79(11)
$\text{S}(3)-\text{S}(2)-\text{C}(2)-\text{C}(1)$	81.97(14)
$\text{S}(2)-\text{C}(2)-\text{C}(3)-\text{C}(4)$	-174.5(2)
$\text{S}(1)-\text{C}(1)-\text{C}(6)-\text{S}(5)$	-179.95(14)

^a Starred atoms are related to the unstarred atoms by symmetry operation: $x, 1/2 - y, z$.

$93.8(1)^\circ$ for the torsion angle $\text{C}-\text{S}-\text{S}$ in **6** is significantly smaller than the corresponding values for the torsion angles involving a central disulfide linkage in **3a** or **3b**, which are in the range $111-118^\circ$. We tentatively suggest that the intermediate detected by ^{19}F NMR in the photochemical transformation of **3a** into **6** is the corresponding boat conformer of **6**.

Conclusions

The 1,2,5,6-tetrathiocins ($\text{C}_6\text{F}_4\text{S}_2$)₂ (**3a**) and ($\text{C}_6\text{Cl}_4\text{S}_2$)₂ (**3b**) adopt chair (C_{2h}) and twist-boat (D_2) conformations of the C_4S_4 ring, respectively. The difference in the energies of the two conformers for **3a** is very small (<5 kJ mol^{-1}), and this derivative undergoes a slow conformational isomerization in solution. The photolysis of **3a** promotes a reversible, transannular sulfur migration to give the 1,2,3,6-isomer (**6**).

Acknowledgements

We thank NSERC (Canada) for financial support, Dr. T. Shimizu for a preprint of ref. 6, and Prof. T.B. Rauchfuss for helpful correspondence and a copy of the Ph.D. thesis of C.P. Galloway in which the possible rearrangement pathway for the transformation of C_6S_{10} into $\text{C}_6\text{S}_8\text{O}_2$ is presented. We also thank Professor C. Langford for the use of photochemical equipment and Professor R. Kydd for his assistance with the measurement of Raman spectra.

References

- Z.S. Herman and K. Weiss. *Inorg. Chem.* **14**, 1592 (1974).
- F.G. Riddell. *In The chemistry of sulphur-containing functional groups*. Edited by S. Patai and Z. Rappoport. John Wiley and Sons, Chichester, U.K. 1993. Chap. 9.

3. (a) C.G. Krespan, B.C. McKusick, and T.L. Cairns. *J. Am. Chem. Soc.* **82**, 1515 (1960); (b) C.G. Krespan. *J. Am. Chem. Soc.* **83**, 3434 (1961).
4. T. Shimizu, K. Iwata, and N. Kamigata. *Angew. Chem. Int. Ed. Engl.* **35**, 2357 (1996).
5. T. Shimizu, K. Iwata, N. Kamigata, and S. Ikuta. *J. Chem. Res. Synop.* 436 (1994).
6. T. Shimizu, K. Iwata, N. Kamigata, and S. Ikuta. *J. Chem. Res. Miniprint*, (1997). In press.
7. X. Yang, T.B. Rauchfuss, and S. Wilson. *J. Chem. Soc. Chem. Commun.* 34 (1990).
8. F. Bigoli, P. Deplano, F.A. Devillanova, J.R. Ferraro, V. Lippolis, P.J. Lukes, M.L. Mercuri, M.A. Pellinghelli, E.F. Trogu, and J.M. Williams. *Inorg. Chem.* **36**, 1218 (1997).
9. (a) G.H. Brooke, B.S. Furniss, W.K.R. Musgrave, and Md.A. Quasem. *Tetrahedron Lett.* 2991 (1965); (b) A. Callaghan, A.J. Layton, and R.S. Nyholm. *J. Chem. Soc. Chem. Commun.* 399 (1969).
10. M.J. Baker-Hawkes, E. Billings, and H.B. Gray. *J. Am. Chem. Soc.* **88**, 21 (1996).
11. R.D. Chambers and D.J. Spring. *Tetrahedron*, **27**, 669 (1971).
12. A.C.T. North, D.C. Phillips, and F.S. Mathews. *Acta Crystallogr. Sect. A: Cryst. Phys. Diffr. Theor. Gen. Crystallogr.* **24**, 351 (1968).
13. A. Altomare, M. Cascarano, C. Giacovazzo, and A. Guagliardi. *SIR92: J. Appl. Crystallogr.* **26**, 343 (1993).
14. P.T. Beurskens, G. Admiraal, G. Beurskens, W.P. Bosman, R. de Gelder, R. Israel, and J.M.M. Smits. *DIRDIF 94: Technical Report of the Crystallography Laboratory*. University of Nijmegen, The Netherlands. 1994.
15. *teXsan: Crystal Structure Analysis Package*. Molecular Structure Corp., The Woodlands, Texas, U.S.A. 1985 and 1992.
16. F. Hai-Fu. *SAPI91: Structure Analysis Program with Intelligent Control*. Rigaku Corp., Tokyo. 1991.
17. G.M. Sheldrick. *SHELXL-93: Program for the Refinement of Crystal Structures*. University of Göttingen, Germany. 1993.
18. T. Chivers, I. Krouse, M. Parvez, I. Vargas-Baca, T. Ziegler, and P. Zoricak. *Inorg. Chem.* **35**, 5836 (1996).
19. R. Steudel. *Angew. Chem. Int. Ed. Engl.* **14**, 655 (1975).
20. H. Wieser, P.J. Krueger, M. Muller, and J.B. Hyne. *Can. J. Chem.* **47**, 1633 (1969).
21. S. Brownridge, T.S. Cameron, J. Passmore, G. Schatte, G.W. Sutherland, and T. Way. *Can. J. Chem.* In press.
22. (a) C.P. Galloway, D.D. Doxsee, D. Fenske, T.B. Rauchfuss, S.R. Wilson, and X. Yang. *Inorg. Chem.* **33**, 4537 (1994); (b) C.P. Galloway. Ph.D. thesis, University of Illinois at Urbana-Champaign. 1994.
23. R. Steudel, Y. Drozdova, K. Miaskiewicz, R.H. Hertwig, and W. Koch. *J. Am. Chem. Soc.* **119**, 1990 (1997).
24. D.N. Harpp, K. Steliou, and C.J. Cheer. *J. Chem. Soc. Chem. Commun.* 825 (1980).
25. (a) L.K. Templeton, D.H. Templeton, and A. Zalkin. *Inorg. Chem.* **15**, 1999 (1976); (b) L.M. Goldsmith and C.E. Strouse. *J. Am. Chem. Soc.* **99**, 7580 (1977).